

Chem, Volume 3

Supplemental Information

**Bifunctional Catalysts for One-Step
Conversion of Syngas into Aromatics
with Excellent Selectivity and Stability**

Kang Cheng, Wei Zhou, Jincan Kang, Shun He, Shulin Shi, Qinghong Zhang, Yang Pan, Wu Wen, and Ye Wang

Supplemental Figures and Tables

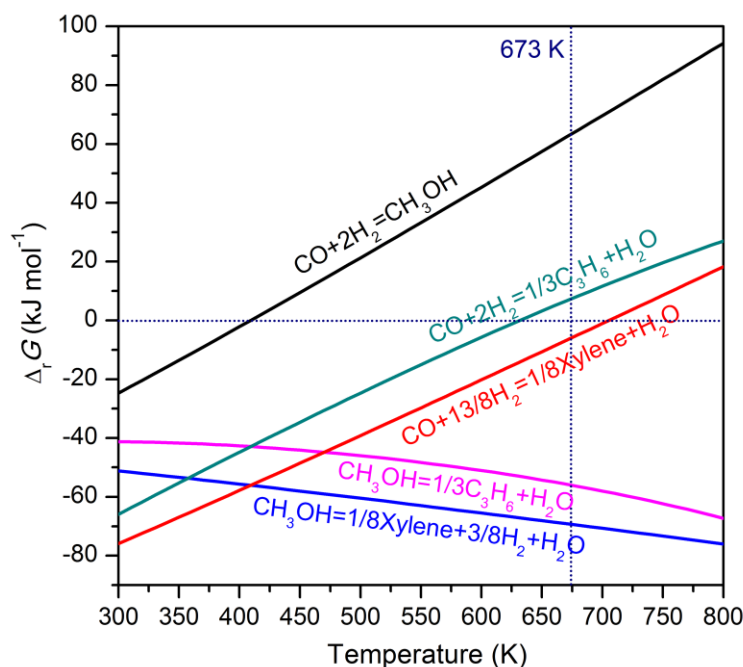


Figure S1. Gibbs free energy changes for several reactions related to the conversion of syngas to aromatics.

The ΔG for the conversion of syngas to methanol is 63 kJ mol^{-1} at 673 K , and thus this reaction is thermodynamically unfeasible at 673 K . On the other hand, the conversion of methanol to aromatics (*p*-xylene as an example) is thermodynamically more favorable at higher temperatures. The ΔG for the conversion of syngas to aromatics (*p*-xylene as an example) is -6.3 kJ mol^{-1} at 673 K . Thus, the MTA reaction can thermodynamically drive the conversion of syngas to aromatics. Furthermore, the conversion of syngas to aromatics is thermodynamically more favorable than the conversion of syngas to olefins.

Table S1. Catalytic performances of some typical catalysts for the conversion of syngas to aromatics.*

Catalyst*	T (K)	CO conv. (%)	Selectivity (%)					
			CH ₄	C ₂₋₄ ^o	C ₂₋₄ ⁼	Aromatics	C ₅₊ ^a	CH ₃ OH/DME
Cu-Zn-Al oxide	623	8.3	20	19	2.4	0	8.6	50
Cu-Zn-Al oxide	703	15	78	16	0.9	0	1.2	3.9
Cu-Zn-Al/H-ZSM-5	623	44	8.2	64	7.9	3.4	16	0.9
Cu-Zn-Al/H-ZSM-5	703	56	11	80	3.8	0.8	4.3	0
Cr-Zn-Al oxide	623	4.4	8.6	13	16	0	18	44
Cr-Zn-Al oxide	703	8.1	66	15	10	0	1.7	6.6
Cr-Zn-Al/H-ZSM-5	623	38	2.1	41	2.4	6.3	48	0
Cr-Zn-Al/H-ZSM-5	703	62	11	65	1.1	1.0	22	0
Zn-ZrO ₂	623	1.0	11	5.2	20	0	11	53
Zn-ZrO ₂	703	5.2	30	11	34	0	14	11
Zn-ZrO ₂ /H-ZSM-5	623	2.8	2.7	9.7	6.5	78	2.9	0
Zn-ZrO ₂ /H-ZSM-5	703	21	2.0	18	4.6	73	2.0	0

*Reaction conditions: catalyst weight, 0.33 g for mixed oxides and 1.0 g for bifunctional catalysts (weight ratio of mixed oxides to H-ZSM-5 = 1:2); H₂/CO = 2:1; 3 MPa; 25 cm³ min⁻¹; time on stream 20 hr. The two components were mixed in an agate mortar for 10 min. ^aC₅₊ denotes aliphatic hydrocarbons with carbon numbers greater than 5.

Table S2. Some typical catalysts capable of catalyzing the formation of aromatics during the conversion of syngas reported in literature.

Catalyst*	T (K)*	P (MPa)	CO conv. (%)	Hydrocarbon selectivity (%)				Ref
				CH ₄	C ₂₋₄	Aromatics	C ₅₊	
Co/SiO ₂ +H-ZSM-5	553+553	2.1	56	15	13	38	34	1
Fe/H-ZSM-5	603	2.0	70	~15	~35	~30	~20	2,3
K-Fe/H-ZSM-5	598	4.5	90	~15	~35	~25	~25	4
Mn-Fe+H-ZSM-5	543+648	1.1	42	19	48	16	17	5
Pd-Fe/H-ZSM-5	583	8.6	76	22	28	32	18	6
Pd/H-ZSM-5	583	8.6	21	20	24	46	10	6
Pd/SiO ₂ +H-ZSM-5	628+628	2.1	17	7.5	52	36	5	7
Pd-Zn-Al/H-ZSM-5	583	6.7	44	9.3	49	22	20	8
Zn-Al/H-ZSM-5	589	5.0	6.7	11	43	33	13	9
Cr-Zn/H-ZSM-5	673	4.0	63	3.7	41	35	21	10

*The two functional components combined using a dual-bed reactor configuration with H-ZSM-5 downstream from a conventional Fischer-Tropsch or methanol-synthesis catalyst were connected with “+”.

Table S3. Related to Figure 1. Detailed product distributions in syngas conversions over Zn-ZrO₂ and Zn-ZrO₂/H-ZSM-5 at different temperatures.*

Catalyst	T (K)	CO conv.(%)	CO ₂ select. (%)	Selectivity of CO hydrogenation products (%)					
				CH ₄	C ₂₋₄ ⁰	C ₂₋₄ ⁼	Aromatics	C ₅₊	CH ₃ OH/DME
Zn-ZrO ₂	573	0.02	10	2.3	7.1	15	0	9.6	66
Zn-ZrO ₂	623	0.82	26	5.6	6.9	19	0	8.5	60
Zn-ZrO ₂	673	2.0	34	8.1	10	21	0	4.9	56
Zn-ZrO ₂	703	2.2	42	13	12	21	0	15	39
Zn-ZrO ₂	723	2.3	37	16	17	22	0	16	29
Zn-ZrO ₂ /H-ZSM-5	573	0.04	16	2	8.2	30	54	6.0	0
Zn-ZrO ₂ /H-ZSM-5	623	0.91	34	1.9	10	19	66	2.4	0
Zn-ZrO ₂ /H-ZSM-5	673	3.4	40	1.7	11	8.8	75	3.2	0
Zn-ZrO ₂ /H-ZSM-5	703	7.6	39	3.5	23	10	58	6.1	0
Zn-ZrO ₂ /H-ZSM-5	723	9.6	36	4.6	30	10	46	10	0

*Reaction conditions: catalyst weight, 0.10 g for Zn-ZrO₂ and 0.30 g for Zn-ZrO₂/H-ZSM-5; 573-723 K; H₂/CO = 2:1; 3 MPa; 25 cm³ min⁻¹; time on stream, 20 hr.

CO₂ is believed to be formed by the water-gas shift reaction (WGS reaction, CO + H₂O → CO₂ + H₂, ΔH₂₉₈⁰ = -41 kJ mol⁻¹) in parallel to the CO hydrogenation. The selectivity of CO₂ was evaluated separately from the hydrogenation of CO. A part of CO conversion was used for CO₂ formation via the WGS reaction and the other part of CO conversion was for the formation of hydrocarbons and/or CH₃OH/DME via CO hydrogenation. The sum of the selectivities of all the products of CO hydrogenation is 100%. The WGS reaction is thermodynamically more favorable at lower temperatures, but the selectivity of CO₂ increases upon increasing the temperature from 573 K to 673 K or 703 K in our case because of the kinetic reason.¹¹ Both ZrO₂ and ZnO were reported to be active for the WGS reaction.^{12,13}

Table S4. Related to Figure 2. Detailed product distributions in syngas conversions over Zn-ZrO₂ and Zn-ZrO₂/H-ZSM-5 at different contact times.*

Catalyst	Contact time (s)	CO conv. (%)	CO ₂ select. (%)	Selectivity of CO hydrogenation products (%)					
				CH ₄	C ₂₋₄ ⁰	C ₂₋₄ ⁼	Aromatics	C ₅₊	CH ₃ OH/DME
Zn-ZrO ₂	0.02	0.30	27	2.8	4.3	10	0	3.6	79
Zn-ZrO ₂	0.08	0.60	32	3.4	4.9	17	0	6.4	68
Zn-ZrO ₂	0.12	0.97	33	3.8	7.3	21	0	8.9	59
Zn-ZrO ₂	0.24	2.0	34	8.1	10	21	0	4.3	56
Zn-ZrO ₂	0.48	3.9	36	16	10	24	0	8.8	41
Zn-ZrO ₂	0.8	5.6	39	22	11	27	0	15	25
Zn-ZrO ₂	1.2	7.7	41	26	11	28	0	17	18
Zn-ZrO ₂	2.4	13	42	30	11	32	0	18	8.8
Zn-ZrO ₂ /H-ZSM-5	0.02	0.40	38	2.6	6.0	53	22	16	0
Zn-ZrO ₂ /H-ZSM-5	0.04	0.80	39	2.7	6.0	35	47	9.6	0
Zn-ZrO ₂ /H-ZSM-5	0.08	1.0	41	2.5	9.1	27	55	6.3	0
Zn-ZrO ₂ /H-ZSM-5	0.12	1.6	42	3.3	10	23	60	3.7	0
Zn-ZrO ₂ /H-ZSM-5	0.24	3.4	41	1.7	11	8.8	75	3.2	0
Zn-ZrO ₂ /H-ZSM-5	0.48	6.0	40	1.6	13	5.6	79	1.7	0
Zn-ZrO ₂ /H-ZSM-5	0.8	9.3	41	1.9	13	2.9	81	1.0	0
Zn-ZrO ₂ /H-ZSM-5	1.2	13	39	1.3	13	2.0	83	0.9	0
Zn-ZrO ₂ /H-ZSM-5	2.4	21	42	2.2	14	2.4	81	0.3	0

*Reaction conditions: catalyst weight, 0.010–3.0 g; 673 K; H₂/CO = 2:1; 3 MPa; 25 cm³ min⁻¹; time on stream, 20 hr.

Table S5. Catalytic performances of Zn-ZrO₂/H-ZSM-5 at different H₂/CO molar ratios.*

H ₂ /CO molar ratio	CO conv. (%)	CO ₂ select. (%)	Hydrocarbon selectivity (%)				
			CH ₄	C ₂₋₄ ⁰	C ₂₋₄ ⁼	Aromatics	C ₅₊
0.5:1	11	38	1.7	8.7	2.8	86	0.6
1:1	14	39	1.8	9.1	2.7	85	1.3
2:1	21	40	2.2	12	2.9	81	2.2
3:1	24	42	2.3	19	2.2	74	2.5

*Reaction conditions: catalyst weight, 3.0 g; 673 K; 3 MPa; 25 cm³ min⁻¹; time on stream, 20 hr.

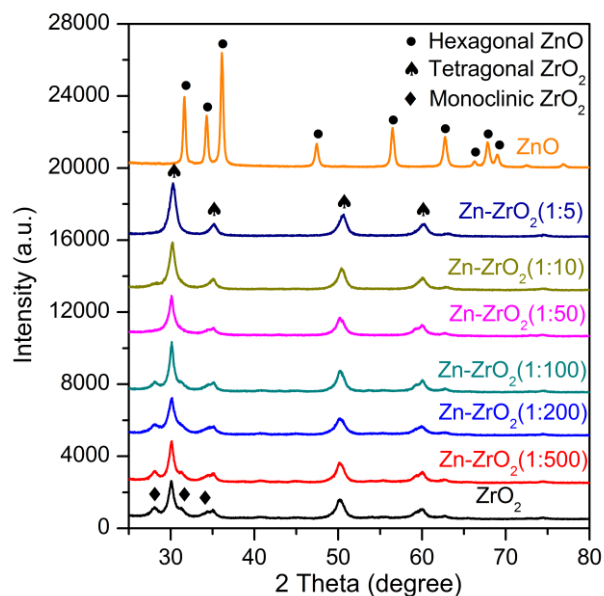


Figure S2. XRD patterns for Zn-ZrO₂ with different Zn/Zr molar ratios.

The number in the parenthesis is the Zn/Zr molar ratio. ZrO₂ was mainly in tetragonal crystalline structure. The doping of a small amount of Zn did not change the crystalline structure of ZrO₂.

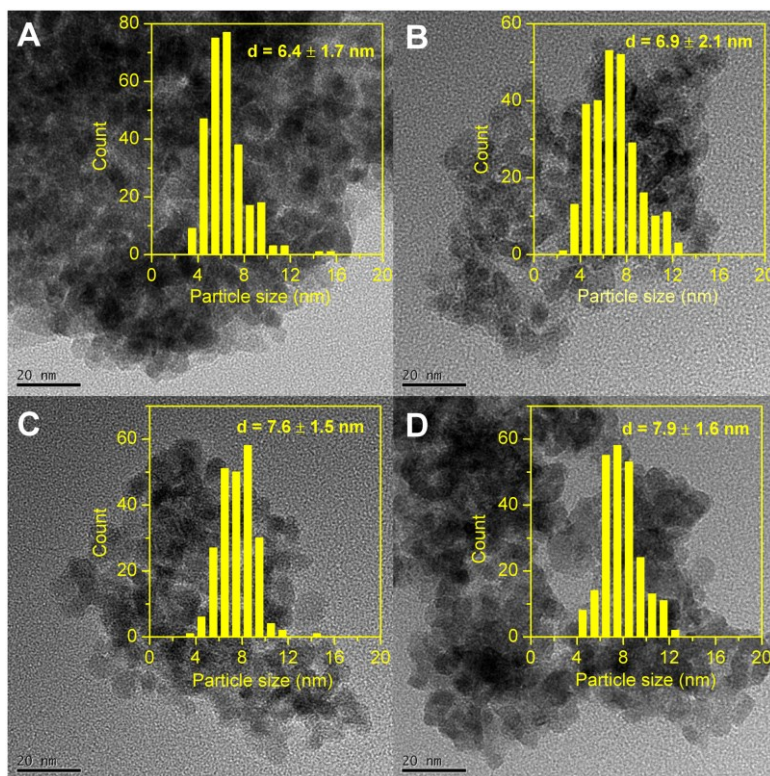


Figure S3. TEM images for Zn-ZrO₂ with different Zn/Zr molar ratios: (A) Zn/Zr = 0, (B) Zn/Zr = 1:200, (C) Zn/Zr = 1:100, (D) Zn/Zr = 1:10. Scale bar, 20 nm.

All the Zn-ZrO₂ samples were composed of nanoparticles with mean sizes <10 nm. The increase in the Zn/Zr molar ratio slightly increased the mean particle size.

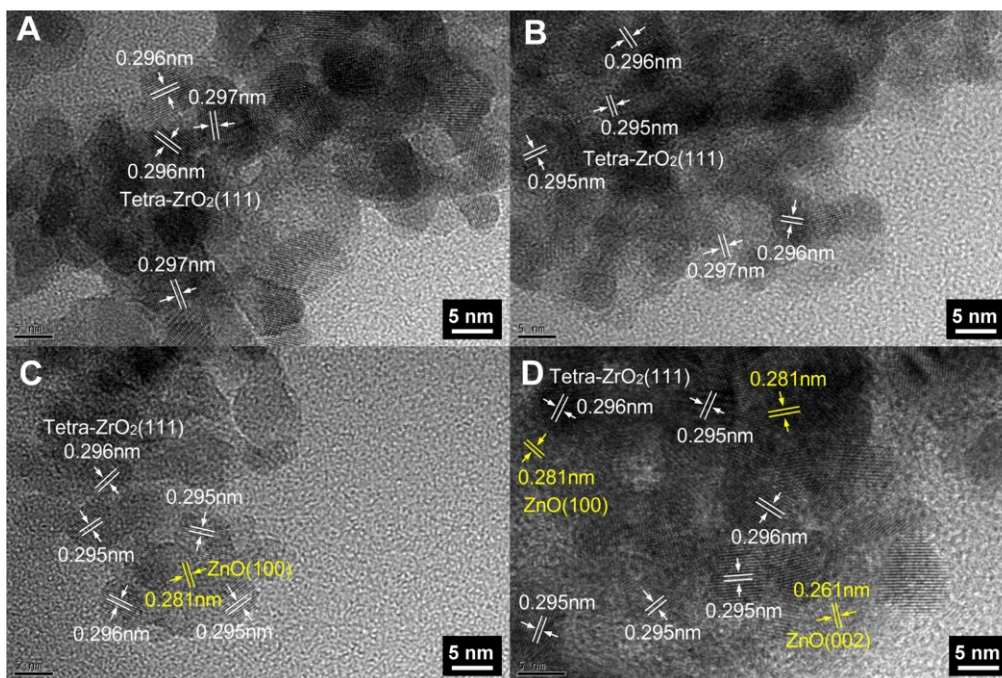


Figure S4. HRTEM images for Zn-ZrO₂ with different Zn/Zr molar ratios: (A) Zn/Zr = 0, (B) Zn/Zr = 1:200, (C) Zn/Zr = 1:100, (D) Zn/Zr = 1:10. Scale bar, 5 nm.

For the Zn-ZrO₂ sample with a Zn/Zr = 1:200, we checked ~200 particles and only observed the lattice fringes belonging to ZrO₂ phase. No ZnO particles were observed, indicating that Zn may be highly dispersed in ZrO₂ as Zn²⁺ or small ZnO clusters. When the Zn/Zr ratio increased to 1:100, the lattice fringes belonging to ZnO particles were observed.

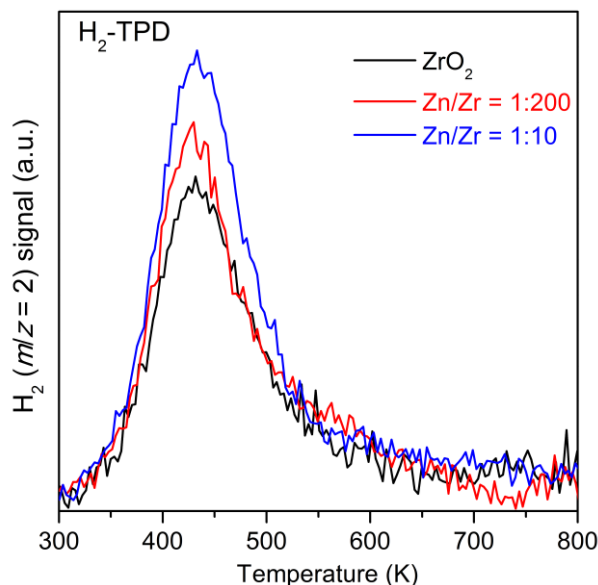


Figure S5. H₂-TPD profiles for Zn-ZrO₂ with different Zn/Zr molar ratios.

The specific surface areas for ZrO₂, Zn-ZrO₂ (Zn/Zr = 1:200) and Zn-ZrO₂ (Zn/Zr = 1:10) were 85, 85 and 71 m² g⁻¹, respectively. All the three samples showed a broad H₂ desorption peak between 300 and 600 K. The addition of Zn species enhanced the adsorption of H₂.

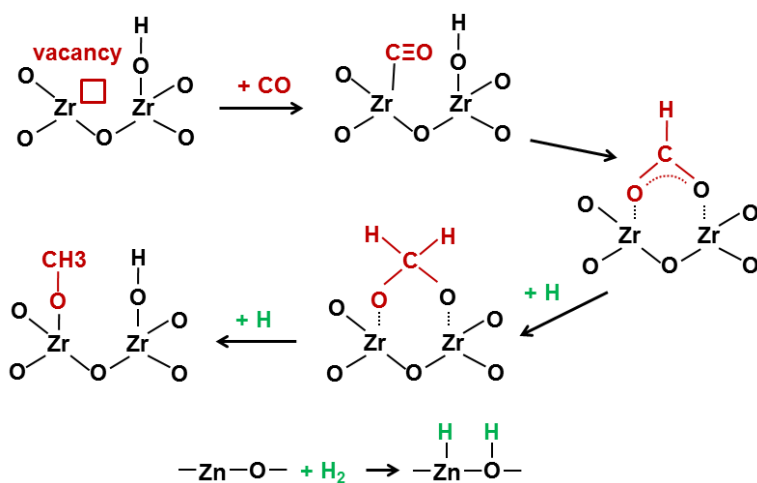


Figure S6. Proposed mechanisms for CO activation on ZrO₂ and for H₂ activation on ZnO surfaces.

Table S6. Catalytic performances of bifunctional catalysts containing Zn-ZrO₂ and zeolites with different topologies for syngas conversions.*

Catalyst	Si/Al ratio ^a	CO conv. (%)	CO ₂ select. (%)	Hydrocarbon selectivity (%)				
				CH ₄	C ₂₋₄ ⁰	C ₂₋₄ ⁼	Aromatics	C ₅₊
Zn-ZrO ₂ /H-ZSM-5	120	9.3	39	1.9	13	2.9	81	1.0
Zn-ZrO ₂ /H-Beta	50	7.5	41	7.5	73	13	4.9	1.8
Zn-ZrO ₂ /H-MOR	12	9.2	40	18	26	43	8.3	4.3
Zn-ZrO ₂ /H-SAPO-34	0.12	7.4	40	4.2	29	61	0.7	5.5

*Reaction conditions: catalyst weight 1.0 g; 673 K; H₂/CO = 2:1; 3 MPa; 25 cm³ min⁻¹; time on stream 20 hr. ^aSi/Al molar ratio was determined by the XRF technique.

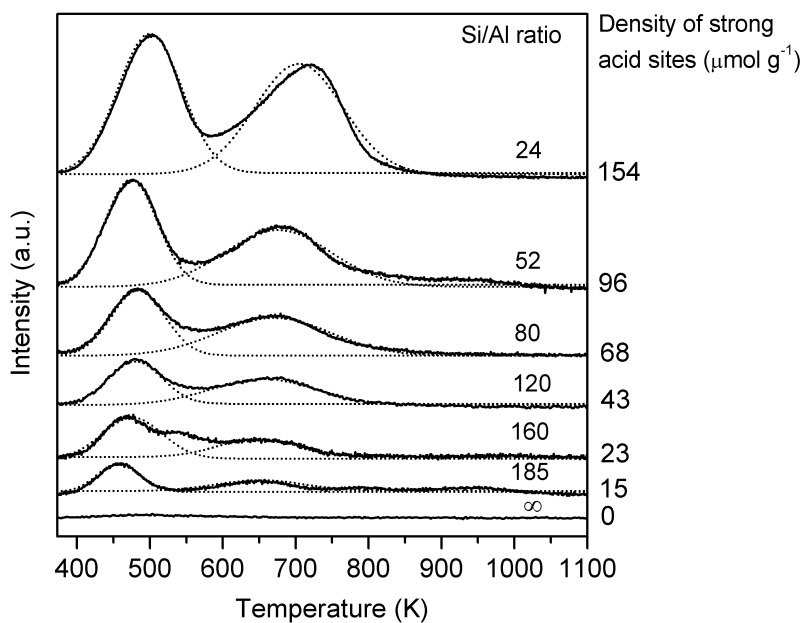


Figure S7. Related to Figure 3B. NH₃-TPD profiles for H-ZSM-5 samples with different Si/Al ratios.

The density of strong acid sites evaluated from the high-temperature peak was displayed in the figure.

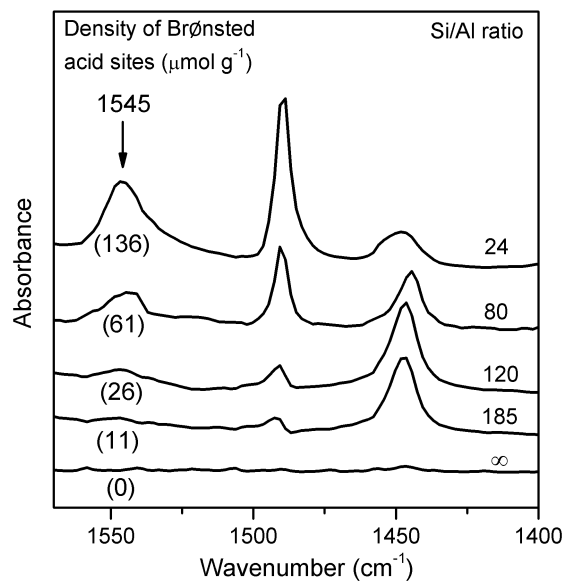


Figure S8. Related to Figure 3B. Pyridine-adsorbed FT-IR spectra for H-ZSM-5 samples with different Si/Al ratios at 423 K.

The numbers in the parentheses are the density of Brønsted acid sites estimated from the IR band at 1545 cm^{-1} belonging to the Brønsted acid site. The extinction coefficient of $\epsilon_B = 1.67 \pm 0.1 \text{ cm mol}^{-1}$ was employed.¹⁴ It is noteworthy that the density of Brønsted acid site evaluated by the pyridine-adsorbed FT-IR may be underestimated, probably because of the large bulk size of pyridine (ca. 5.5 Å) and its steric limitation, which leads to the difficulty to access all the acid sites in H-ZSM-5 by pyridine molecules.^{15,16}

Table S7. Catalytic performances of bifunctional catalysts with different weight ratios of Zn-ZrO₂ to H-ZSM-5.*

Zn-ZrO ₂ /H-ZSM-5 weight ratio	CO conv. (%)	CO ₂ select. (%)	Hydrocarbon selectivity (%)				
			CH ₄	C ₂₋₄ ⁰	C ₂₋₄ ⁼	Aromatics	C ₅₊
2:1	32	41	1.9	21	8.8	61	7.4
1:1	25	39	1.7	18	7.8	67	5.7
1:2	21	41	2.0	18	4.6	73	2.0
1:4	16	42	2.0	21	4.9	70	2.0

*Reaction conditions: catalyst weight, 1.0 g; 703 K; H₂/CO = 2:1; 3 MPa; 25 $\text{cm}^3 \text{ min}^{-1}$; time on stream, 20 hr.

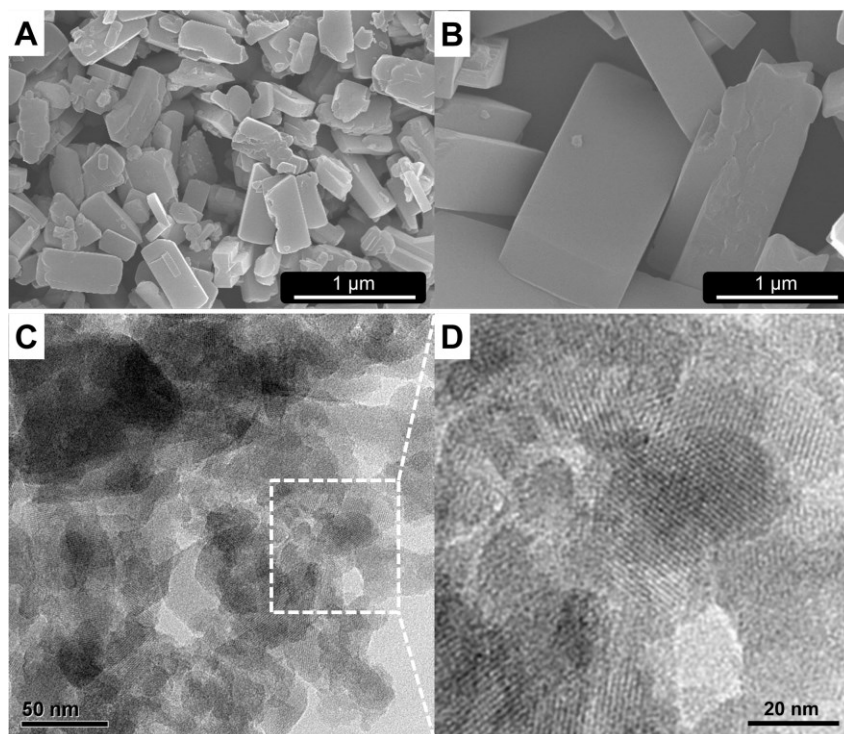


Figure S9. Related to Figure 4. (A, B) SEM images for the micro-sized H-ZSM-5. Scale bar, 1 μm . (C, D) TEM images for the nano-sized H-ZSM-5. Scale bars, 50 nm for (C) and 20 nm for (D).

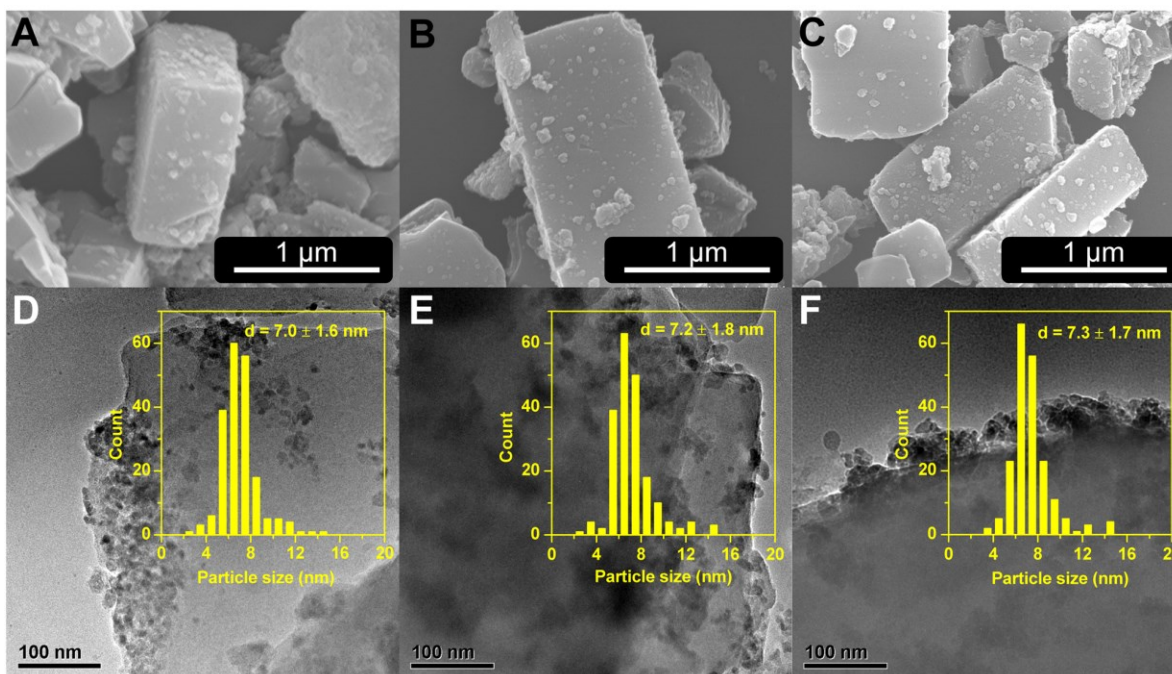


Figure S10. SEM images for the bifunctional Zn-ZrO₂/H-ZSM-5 catalyst after reactions for different times: (A) Fresh, (B) 50 hr, (C) 100 hr. Scale bar, 1 μm . TEM images and corresponding size distributions of Zn-ZrO₂ particles for the bifunctional Zn-ZrO₂/H-ZSM-5 catalyst after reaction for different times: (A) Fresh, (B) 50 hr, (C) 100 hr. Scale bar, 100 nm.

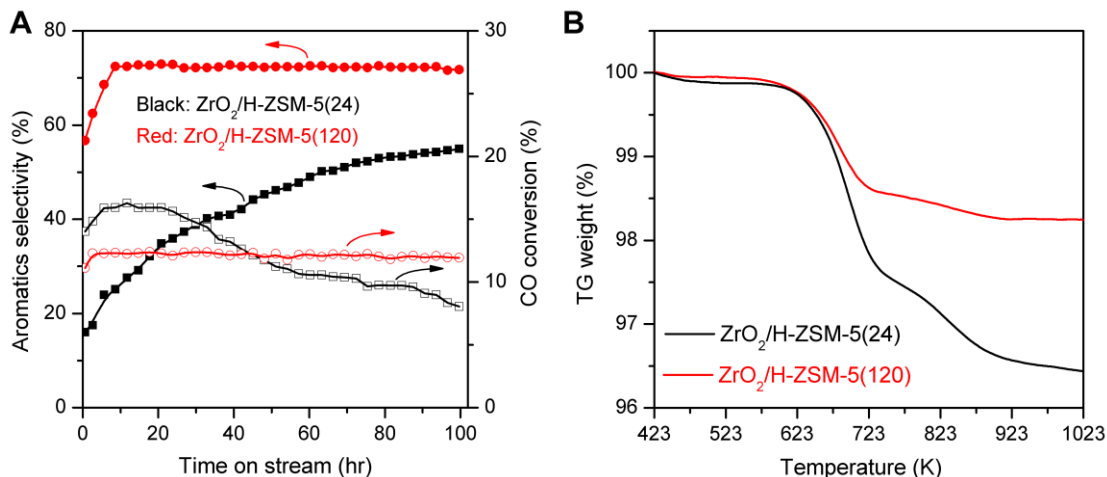


Figure S11. (A) Catalytic performances of ZrO₂/H-ZSM-5 catalysts with different Si/Al ratios (in parenthesis) for syngas conversions. Reaction conditions: catalyst weight, 1.0 g; 703 K; H₂/CO = 2:1; 3 MPa; 25 cm³ min⁻¹. (B) Thermogravimetry analysis of ZrO₂/H-ZSM-5(24) and ZrO₂/H-ZSM-5(120) catalysts after 100 hr reactions in air.

The ZrO₂/H-ZSM-5(120) with an appropriate density of strong acid sites displayed very stable catalytic performances, whereas the ZrO₂/H-ZSM-5(24) with a higher density of strong acid sites suffered from faster deactivation. The selectivity of aromatics over the ZrO₂/H-ZSM-5(24) increased gradually along with a decrease in CO conversion, possibly because some strong acid sites that could catalyze the hydrogenation of lower olefins to lower paraffins were covered by the coke deposited. The thermogravimetry analysis showed that the amount of carbon deposited on the ZrO₂/H-ZSM-5(120) after 100 hr reaction was 18 mg g_{cat}⁻¹, which was much lower than that on the ZrO₂/H-ZSM-5(24) after 100 hr reaction (37 mg g_{cat}⁻¹).

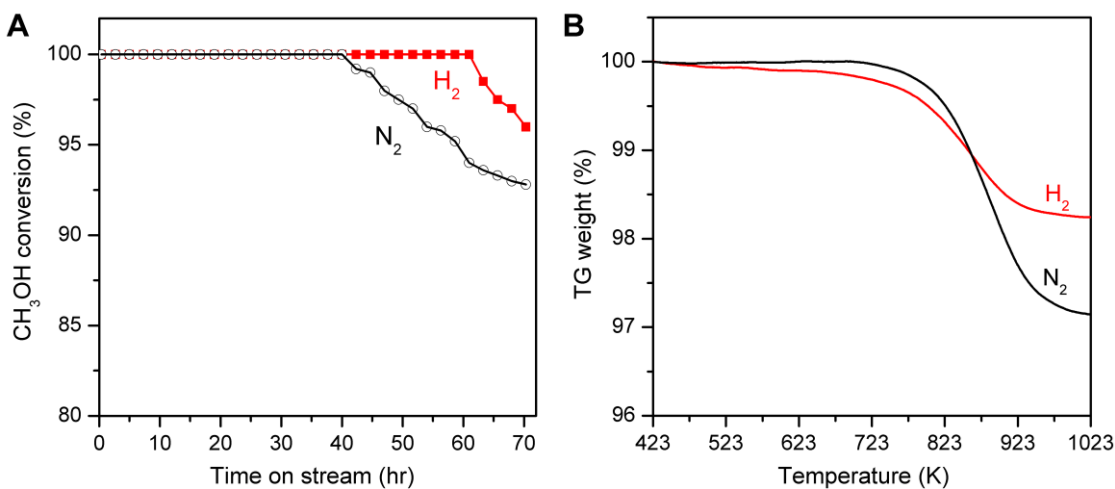


Figure S12. (A) Effect of the atmosphere on the stability for the conversion of methanol over H-ZSM-5. (B) Thermogravimetry analysis of the H-ZSM-5 after the conversion of methanol for 20 hr. Reaction conditions: catalyst weight, 1.0 g; 673 K; liquid CH₃OH flow rate, 4.8 cm³ hr⁻¹; gas (N₂ or H₂) flow rate, 25 cm³ min⁻¹.

Under N₂ atmosphere, the MTA reaction began to deactivate at 40 hr, while the catalyst stability was significantly improved under H₂. The thermogravimetry analysis showed that the amount of carbon deposited on H-ZSM-5 catalyst under H₂ atmosphere was 18 mg g_{cat}⁻¹, lower than that under N₂ (31 mg g_{cat}⁻¹).

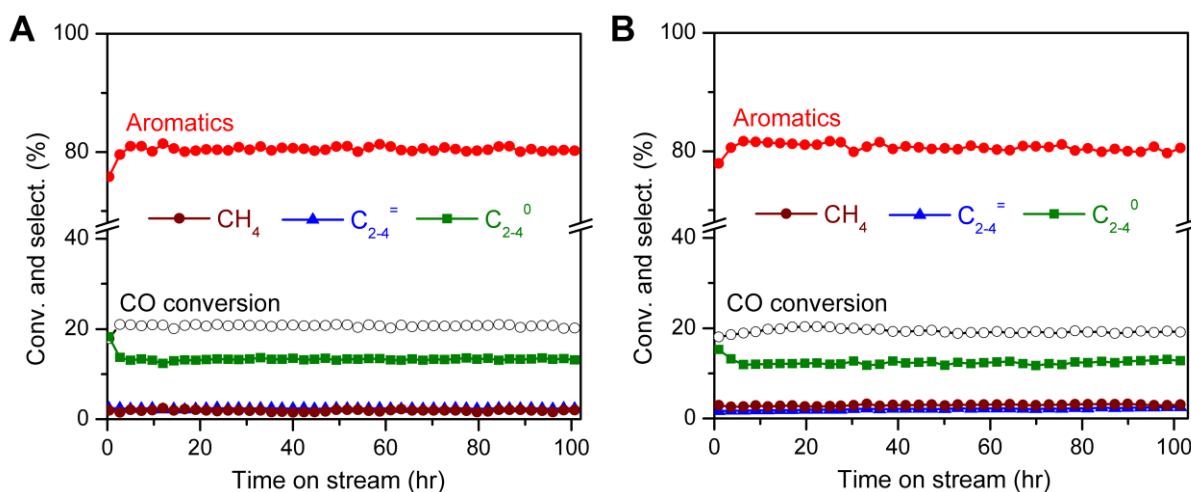


Figure S13. (A) Stability of the Zn-ZrO₂/H-ZSM-5 catalyst for the conversion of 1.0 vol % CO₂-containing syngas. Reaction conditions: catalyst weight, 3.0 g; 673 K; H₂/CO/CO₂/Ar = 64:32:1:3; 3 MPa; 25 cm³ min⁻¹. (B) Stability of the Zn-ZrO₂/H-ZSM-5 catalyst for the conversion of 10 ppm H₂S-containing syngas. Reaction conditions: catalyst weight, 3.0 g; 673 K; H₂/CO = 2:1; H₂S, 10 ppm; 3 MPa; 25 cm³ min⁻¹.

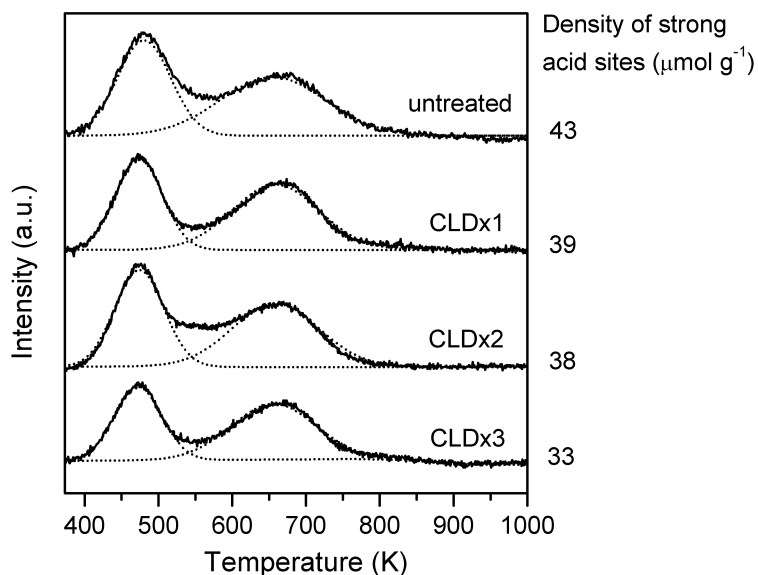


Figure S14. Related to Figure 6. NH₃-TPD profiles for TEOS-modified H-ZSM-5 by the CLD method.

The NH₃-TPD quantitative results showed that the silylation by TEOS caused gradual decrease in the density of strong acid sites. The modification preferentially passivated the Brønsted acid sites located on the external surfaces and in the pore-mouth region of H-ZSM-5.¹⁷ Thus, we speculated that the slight decrease in the total density of strong acid sites evaluated by NH₃-TPD was probably due to the selective passivation of the Brønsted acid sites by CLD treatment.

Table S8. Related to Figure 6. Catalytic performances of Zn-ZrO₂/H-ZSM-5 catalysts with H-ZSM-5 modified by TEOS with the CLD method.*

Cycles of CLD treatment	CO conv. (%)	Hydrocarbon selectivity (%)				
		CH ₄	C ₂₋₄ ⁰	C ₂₋₄ ⁼	Aromatics	C ₅₊
0	21	2.0	18	4.6	73	2.0
1	19	1.5	16	5.6	76	1.8
2	19	1.6	18	4.9	73	2.2
3	18	1.5	17	4.8	74	2.0

*Reaction conditions: catalyst weight, 1.0 g; 703 K; 3 MPa; H₂/CO = 2:1; 25 cm³ min⁻¹; time on stream, 20 hr.

Table S9. Effect of gaseous atmosphere and pressure on product selectivity during methanol conversion.*

Catalyst	Atmosphere	P (MPa)	CH ₃ OH conv. (%)	Hydrocarbon selectivity (%)				
				CH ₄	C ₂₋₄ ⁰	C ₂₋₄ ⁼	Aromatics	C ₅₊
H-ZSM-5	N ₂	0.1	100	1.0	20	46	21	13
H-ZSM-5	H ₂	0.1	100	1.2	28	39	21	11
H-ZSM-5	CO	0.1	100	1.3	25	42	22	9.4
Zn-ZrO ₂ /H-ZSM-5	N ₂	0.1	100	1.1	21	52	18	8.2
Zn-ZrO ₂ /H-ZSM-5	H ₂	0.1	100	1.0	29	45	19	6.2
Zn-ZrO ₂ /H-ZSM-5	CO	0.1	100	1.1	22	35	34	7.4
Zn-ZrO ₂ /H-ZSM-5	CO	0.5	100	1.9	22	18	52	5.3
Zn-ZrO ₂ /H-ZSM-5	CO	1.0	100	2.0	22	5.5	70	1.0
Zn-ZrO ₂ /H-ZSM-5	CO	2.0	100	1.6	22	1.2	75	0.6

*Reaction conditions: catalyst weight, 1.0 g; 673 K; liquid CH₃OH flow rate, 0.06 cm³ hr⁻¹; gas (N₂, H₂ or CO) flow rate, 6 cm³ min⁻¹; time on stream, 20 hr.

Table S10. Effect of H-ZSM-5 sizes on the conversion of methanol over bifunctional catalysts.*

Catalyst	CH ₃ OH conv. (%)	Hydrocarbon selectivity (%)				
		CH ₄	C ₂₋₄ ⁰	C ₂₋₄ ⁼	Aromatics	C ₅₊
Zn-ZrO ₂ /micro-H-ZSM-5	100	1.1	21	52	18	8.2
Zn-ZrO ₂ /nano-H-ZSM-5	100	1.9	22	47	22	7.0

*Reaction conditions: catalyst weight, 1.0 g; 673 K; liquid CH₃OH flow rate, 0.06 cm³ hr⁻¹; N₂ flow rate, 6 cm³ min⁻¹; time on stream, 20 hr.

Table S11. Effect of gaseous atmosphere and pressure at elevated gas flow rate on product selectivity during methanol conversion.*

Catalyst	Atmosphere	P (MPa)	CH ₃ OH conv. (%)	Hydrocarbon selectivity (%)				
				CH ₄	C ₂₋₄ ⁰	C ₂₋₄ ⁼	Aromatics	C ₅₊
Zn-ZrO ₂ /H-ZSM-5	N ₂	0.1	100	0.3	23	61	8.0	7.6
Zn-ZrO ₂ /H-ZSM-5	CO	0.1	100	0.6	21	56	16	6.0
Zn-ZrO ₂ /H-ZSM-5	CO	1.0	100	0.5	24	12	60	3.2

*Reaction conditions: catalyst weight, 1.0 g; 673 K; liquid CH₃OH flow rate, 0.06 cm³ hr⁻¹; gas (N₂ or CO) flow rate, 25 cm³ min⁻¹; time on stream, 20 hr.

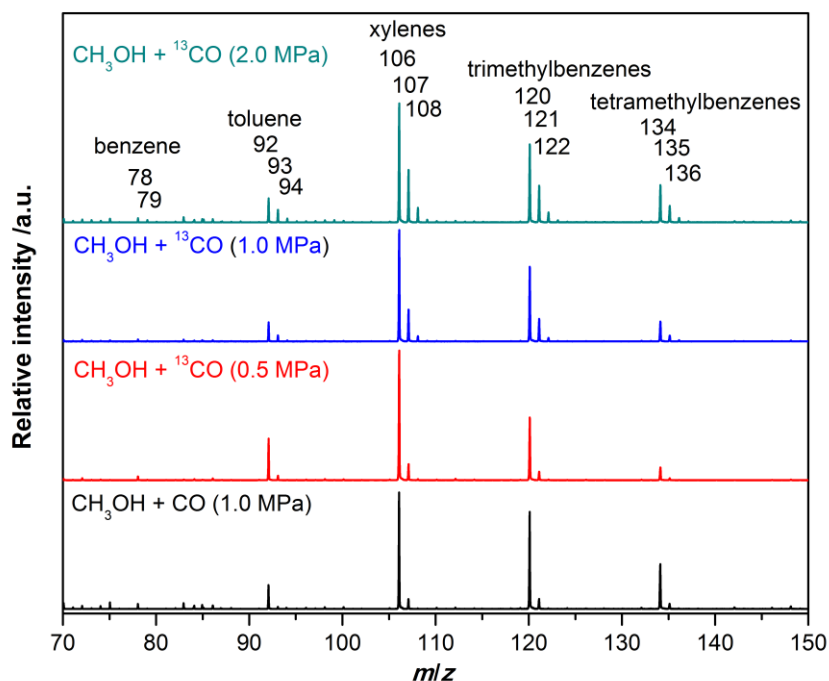


Figure S15. Related to Figure 7C. Results from synchrotron-based vacuum ultraviolet photoionization mass spectrometry for hydrocarbon products collected from the conversion of CH_3OH under CO or ^{13}CO with different pressures over $\text{Zn-ZrO}_2/\text{H-ZSM-5}$ catalyst.

Signals of $m/z = 78$ (^{12}C -benzene), 92 (^{12}C -toluene), 106 (^{12}C -xylenes), 120 (^{12}C -trimethylbenzenes) and 134 (^{12}C -tetramethylbenzenes) were detected at a photon energy of 10.6 eV. Signals of $m/z = 79, 93, 94, 107, 108, 121, 122, 135, 136$ were unambiguously attributed to ^{13}C -containing products of benzene, toluene, xylenes, trimethylbenzenes and tetramethylbenzenes, respectively. The intensity is proportional to the concentration.

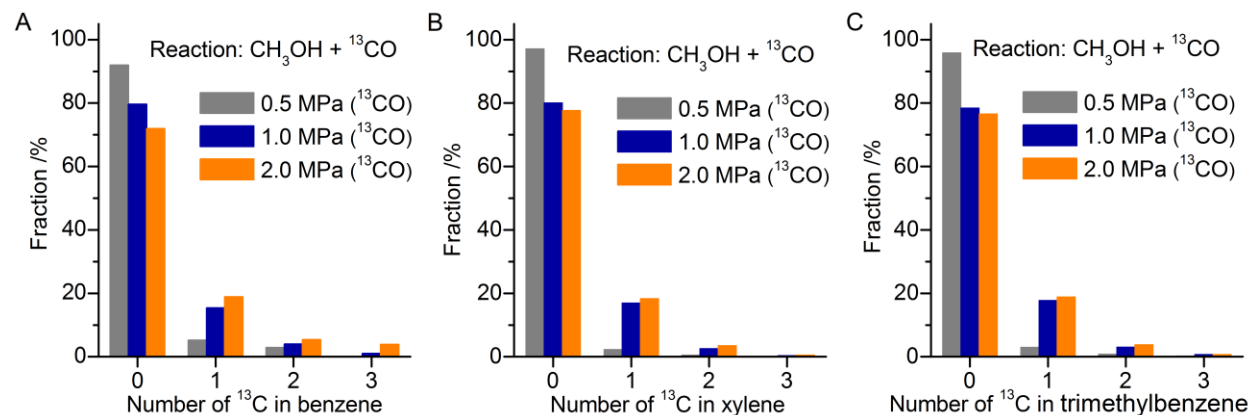


Figure S16. Related to Figure 7C. Incorporation of ^{13}C into aromatic products during the conversion of CH_3OH under ^{13}CO . (A) Benzene. (B) Xylenes. (C) Trimethylbenzenes.

The amount of ^{13}C incorporated into aromatic products increased with ^{13}CO pressure.

Table S12. Comparison of productivities for the formation of aromatics in different processes.

Catalysts	Reactant	Reaction conditions	Conv. (%)	Product selectivity (%)	Productivity (g g _{cat} ⁻¹ h ⁻¹)	Stability	Ref.
Optimized catalyst	Syngas	703 K/4 MPa	23	80 ^a	0.12 ^a	Stable in 1000 hr	This work
Mo/ZSM-5	Methane	973 K/0.1 MPa	10-12	~75 ^a	~0.04 ^a	Unstable in 5 hr	18
Zn/P/ZSM-5	Methanol	748 K/0.1 MPa	100	76 ^a	~0.2 ^a	Unstable in 6 hr	19
Ga/ZSM-5	Propane	813 K/0.1 MPa	38	50 ^a	~0.6 ^a	Unstable in 4.5 hr	20
CuZnAl	Syngas	518 K/4.5 MPa	~20	99 ^b	1.3 ^b	Stable	21,22

^aAromatics. ^bMethanol.

Supplemental Experimental Procedures:

Synthesis of Zn-ZrO₂ nanoparticles. Zn-ZrO₂ nanoparticles were synthesized by a hard-template method.²³ Typically, Zr(NO₃)₄·5H₂O (8.0 g) was dissolved in distilled water (15 cm³), and then the aqueous solution of Zn(NO₃)₂ with stoichiometric amount was added into the solution of Zr(NO₃)₄ by a liquid-moving gun. Subsequently, carbon black (2.0 g), which was used as a hard template, was added into the solution. The mixture was stirred at 343 K for 5 hr, followed by drying in a vacuum oven overnight at 333 K. The precursor was calcined in air at 773 K for 10 hr, resulting white-powdery product. The elemental analysis showed that carbon had been removed by calcination. The typical Zn/Zr molar ratio in Zn-ZrO₂ nanoparticles was 1:200 unless otherwise mentioned. ZrO₂ was also prepared with the same procedure except for without the addition of Zn(NO₃)₂.

Synthesis of Cu-Zn-Al and Cr-Zn-Al oxides. For comparison, Cr-Zn-Al (Cr/Zn/Al = 2:7:2, molar ratio) and Cu-Zn-Al (Cu/Zn/Al = 6:3:1, molar ratio) oxides were prepared by a co-precipitation method.²⁴ For the preparation of Cr-Zn-Al oxide, 14.56 g Zn(NO₃)₂·6H₂O, 5.6 g Cr(NO₃)₃·9H₂O and 5.25 g Al(NO₃)₃·9H₂O were dissolved in 100 cm³ distilled water. The aqueous solution of (NH₄)₂CO₃ was used as the precipitant and was added into the mixed aqueous solution for precipitation at 343 K. The obtained precipitate was aged for 3 hr at 343 K, followed by filtration and washing with deionized water. The solid product was then dried at 383 K overnight and calcined in air at 773 K for 1 hr. The Cu-Zn-Al oxide was prepared with the same procedure.

Treatment of H-ZSM-5. Zeolite H-ZSM-5 samples with different Si/Al molar ratios were purchased from Nankai University Catalyst Co. Typically, H-ZSM-5 with a Si/Al ratio of 120 was used unless otherwise mentioned. The silylation of H-ZSM-5 (Si/Al = 120) was carried out by a chemical liquid deposition (CLD) method.¹⁷ In brief, H-ZSM-5 (4.0 g) was suspended in 100 cm³ hexane and the mixture was heated with stirring until reflux conditions. Then, 0.6 cm³ tetraethoxysilane (TEOS) was introduced into the mixture and the silylation was carried out for 1 hr under reflux conditions. Subsequently, hexane was removed by evacuation. The samples were dried at 393 K for 2 hr and calcined in air at 773 K for 4 hr. The CLD was performed repeatedly for several cycles using the calcined sample.

Synthesis of Nano-sized H-ZSM-5. Nano-sized H-ZSM-5 (Si/Al = 120) was synthesized by a hydrothermal method in the presence of 3-[(trimethoxysilyl)propyl]hexadecyldimethylammonium chloride (TPHAC).²⁵ In brief, 11.9 g TPHAC (64 wt% in methanol) and 85.7 g TEOS were dissolved under vigorous stirring in a solution consisting of 28.0 g tetrapropyl ammonium bromide, 8.0 g NaOH, 0.28 g NaAlO₂ and 1350 g water at room temperature. The resultant mixture was aged at room temperature overnight while keeping stirring. The synthesis mixture was transferred into a Teflon-coated stainless steel autoclave and was subjected to hydrothermal treatment at 443 K for 3 d under stirring. After cooling to room temperature, the zeolite product was recovered by filtration and washed thoroughly with deionized water. The product was dried overnight at 373 K and subsequently calcined in air at 823 K for 5 hr. The Na-form zeolite was further exchanged with NH₄NO₃ aqueous solution (1.0 M) for three times to obtain the H-form nano-sized ZSM-5.

Preparation of bifunctional catalyst. The bifunctional catalyst was typically prepared by physical mixing. The mass ratio of the two components (Zn-ZrO₂ and H-ZSM-5) was fixed at 1:2 in this work. The two components were mixed in an agate mortar for 10 min. The nanocomposite of Zn-ZrO₂ and H-ZSM-5 was prepared with the same procedure except for using nano-sized H-ZSM-5 instead of H-ZSM-5 crystallites. For the preparation of the Zn-ZrO₂/H-ZSM-5 composed of mixed granules, the powdery Zn-ZrO₂ and H-ZSM-5 were preliminarily pressed, crushed and sieved to granules of 30-60 meshes (sizes, 250-600 μm), respectively. Then, the granules of the two samples were simply mixed together by shaking in a vessel.

Catalytic reaction. The syngas conversion was performed on a high-pressure fixed-bed flow reactor designed by Xiamen HanDe Engineering Co., Ltd. Typically, the catalyst (1.0 or 3.0 g) with grain sizes of 250-600 μm (30-60 mesh) was loaded in a titanium reactor (inner diameter, 10 mm). The syngas with a H₂/CO ratio of 2:1 was employed in this work and Ar with a concentration of 4% contained in the syngas was used as an internal standard for the calculation of CO conversion. The flow rate of syngas was manipulated at 25 cm³ min⁻¹ (293 K, 101 kPa) for each reaction. The syngas pressure and the reaction temperature were typically 3.0 MPa and 703 or 673 K, respectively. The product selectivity was calculated on a molar carbon basis for CO hydrogenation. The MTA reaction was performed in the same

reactor, and liquid methanol ($0.060 \text{ cm}^3 \text{ hr}^{-1}$) was fed into the reactor by a Series III Pump with N_2 or CO gas flow ($6 \text{ cm}^3 \text{ min}^{-1}$). The catalytic performances after 20 hr were typically used for discussion.

Products were analyzed by online gas chromatographs (Ruimin GC2060, Shanghai), which were equipped with a thermal conductivity detector (TCD) and two flame ionization detectors (FID). TDX-01 packed column was connected to TCD, while HP-Pona and Rt-Q-BOND-PLOT capillary columns were connected to FID. The product selectivity was calculated on a molar carbon basis.

Isotopic tracing study on the conversion of CH_3OH under ^{13}CO . The isotopic tracing study was carried out in a closed titanium microreactor with 10 mm inner diameter and 50 cm^3 dead volume. The $\text{Zn-ZrO}_2/\text{H-ZSM-5}$ catalyst (1.0 g) was first placed in the middle of the reactor between quartz-wool plugs. Then, 0.8 g of liquid CH_3OH was introduced into the reactor. The reactor was purged three times with ^{13}CO and was then sealed at a ^{13}CO pressure of 0.5-2.0 MPa. The reactor was kept at 673 K for 3 hr. After the reactor was cooled to room temperature, the liquid products were extracted by CH_2Cl_2 solvent.

The analysis of ^{13}C distributions in aromatic hydrocarbons was carried out at the Mass Spectrometry beamline of the National Synchrotron Radiation Laboratory at Hefei, China. The volatile components of collected products in CH_2Cl_2 were directly introduced into the ionization chamber through a heated deactivated fused-silica capillary, and were analyzed using synchrotron-based vacuum ultraviolet photoionization mass spectrometry (SVUV-PIMS), which can provide fragment-free mass spectra with high sensitivity.^{26,27} The fractions of aromatics with different ^{13}C numbers were calculated by subtracting the isotopic abundances.

Catalytic characterization. X-ray fluorescence (XRF) spectroscopy, which could provide information of elemental compositions of Si and Al, was measured with a Panalytical Axois Petro XRF instrument with rhodium target (50 kV, 50 mA). The content of carbon in the mixed Zn-ZrO_2 oxides was determined by Vario EL III elemental analyzer (Elementar Analysen System GmbH). X-ray diffraction (XRD) patterns were recorded on a Rigaku Ultima IV diffractometer (Rigaku, Japan). $\text{Cu } K_\alpha$ radiation (40 kV and 30 mA) was used as the X-ray source. Transmission electron microscopy (TEM) measurements were performed on a Phillips Analytical FEI Tecnai 20 electron microscope operated at an acceleration voltage of 200 kV. The sample was dispersed ultrasonically in ethanol for 5 min, and a drop of solution was deposited onto a carbon-coated copper grid. Scanning electron microscopy (SEM) measurements were carried out using a ZEISS SIGMA scanning electron microscope with 20 kV accelerating voltage. H_2 temperature-programmed desorption (H_2 -TPD) was measured on a Micromeritics AutoChemII 2920 instrument. Typically, 500 mg of samples were used for each measurement. The sample was pretreated at 773 K in an O_2 -He gas (20 vol % O_2) flow for 60 min. Then, the gas flow was switched to H_2 and the sample was cooled to at 298 K for 6 hr under H_2 . The gaseous and weakly adsorbed H_2 were subsequently removed by purge with He for an additional 60 min. Subsequently, the temperature was raised from 298 to 800 K at a rate of 30 K min^{-1} and the H_2 -TPD profile was recorded by a mass spectrometer with a signal of $m/z = 2$. Thermogravimetric (TG) analysis was performed in air flow on a SDT-Q600 apparatus. The sample was dried at 423 K for 2 hr, then heated to 1073 K at a rate of 10 K min^{-1} . NH_3 temperature-programmed desorption (NH_3 -TPD) measurements were performed on a Micromeritics AutoChemII 2920 instrument. Typically, the sample was pretreated in a quartz reactor with an O_2 -He gas (20 vol % O_2) flow at 673 K for 60 min, followed by purge with high-purity He. The adsorption of NH_3 was performed at 373 K in an NH_3 -He mixture (10 vol % NH_3) for 60 min, and TPD was performed in He flow by raising the temperature to 1173 K at a rate of 10 K min^{-1} . Pyridine (Py) and 2,6-di-tert-butyl-pyridine (2,6-DTBPY) adsorbed FT-IR studies were performed with a Nicolet 6700 instrument equipped with an MCT detector. The sample was pressed into a self-supported wafer and placed in an *in situ* IR cell. After pretreatment under vacuum at 773 K for 60 min, the sample was cooled to 423 K. Spectra of degassed samples were collected as background. Then, Py or 2,6-DTBPY was adsorbed at 423 K onto the sample for a sufficient time.

Supplemental References:

1. Gormley, R. J., Rao, V. U. S., Anderson, R. R., Schehl, R. R., Chi, R. D. H. (1988). Secondary reactions on metal-zeolite catalysts used in synthesis gas conversion. *J. Catal.* **113**, 193-205.
2. Botes, F. G. (2005). The effect of a higher operating temperature on the Fischer–Tropsch/HZSM-5 bifunctional process. *Appl. Catal. A* **284**, 21-29.
3. Botes, F. G., Böhringer, W. (2004). The addition of HZSM-5 to the Fischer–Tropsch process for improved gasoline production. *Appl. Catal. A* **267**, 217-225.
4. Schulz, H., Niederberger, H. L., Kneip, M., Weil, F. (1991). Synthesis Gas Conversion on Fischer–Tropsch Iron/HZSM5 Composite Catalysts. *Stud. Surf. Sci. Catal.* **61**, 313-323.
5. Baerns, M., Guan, N., Körting, E., Lindner, U., Lohrengel, M., Papp, H. (1994). Catalyst development for selective conversion of syngas to mainly aromatic hydrocarbons. *Int. J. Energ. Res.* **18**, 197-204.
6. Yan, Q., Lu, Y., Wan, C., Han, J., Rodriguez, J., Yin, J., Yu, F. (2014). Synthesis of Aromatic-Rich Gasoline-Range Hydrocarbons from Biomass-Derived Syngas over a Pd-Promoted Fe/HZSM-5 Catalyst. *Energ. Fuel* **28**, 2027-2034.
7. Fujimoto, K., Kudo, Y., Tominaga, H. (1984). Synthesis gas conversion utilizing mixed catalyst composed of CO reducing catalyst and solid acid: II. Direct synthesis of aromatic hydrocarbons from synthesis gas. *J. Catal.* **87**, 136-143.
8. Dagle, R. A., Lizarazo-Adarme, J. A., Lebarbier Dagle, V., Gray, M. J., White, J. F., King, D. L., Palo, D. R. (2014). Syngas conversion to gasoline-range hydrocarbons over Pd/ZnO/Al₂O₃ and ZSM-5 composite catalyst system. *Fuel Process. Technol.* **123**, 65-74.
9. Chang, C. D., Lang, W. H., Silvestri, A. J., Smith, R. L. (1978) U. S. Patent 4096163.
10. Ereña, J., Arandes, J. M., Bilbao, J., Aguayo, A. T., de Lasa, H. I. (1998). Study of Physical Mixtures of Cr₂O₃–ZnO and ZSM-5 Catalysts for the Transformation of Syngas into Liquid Hydrocarbons. *Ind. Eng. Chem. Res.* **37**, 1211-1219.
11. Choi, Y., Stenger, H. G. (2003). Water gas shift reaction kinetics and reactor modeling for fuel cell grade hydrogen. *J. Power Sources* **124**, 432-439.
12. Kouva, S., Andersin, J., Honkala, K., Lehtonen, J., Lefferts, L., Kanervo, J. (2014). Water and carbon oxides on monoclinic zirconia: experimental and computational insights. *Phys. Chem. Chem. Phys.* **16**, 20650-20664.
13. Rethwisch, D. G., Dumesic, J. A. (1986). Adsorptive and catalytic properties of supported metal oxides III. Water–Gas Shift over Supported Iron and Zinc Oxides. *J. Catal.* **101**, 35-42.
14. Koo, J.-B., Jiang, N., Saravanamurugan, S., Bejblova, M., Musilova, Z., Čejka, J., Park, S.-E. (2010). Direct synthesis of carbon-templating mesoporous ZSM-5 using microwave heating. *J. Catal.* **276**, 327-334.
15. Choi, S.-W., Kim, W.-G., So, J. S., Moore, J. S., Liu, Y., Dixit, R. S., Pendergast, J. G., Sievers, C., Sholl, D. S., Nair, S., Jones, C. W. (2017). Propane dehydrogenation catalyzed by gallosilicate MFI zeolites with perturbed acidity. *J. Catal.* **345**, 113-123.
16. Bludau, H., Karge, H. G., Niessen, W. (1998). Sorption, sorption kinetics and diffusion of pyridine in zeolites. *Microporous and Mesoporous Materials* **22**, 297-308.
17. Zheng, S., Heydenrych, H. R., Jentys, A., Lercher, J. A. (2002). Influence of Surface Modification on the Acid Site Distribution of HZSM-5. *J. Phys. Chem. B* **106**, 9552-9558.
18. Kosinov, N., Coumans, F. J. A. G., Uslamin, E. A., Wijpkema, A. S. G., Mezari, B., Hensen, E. J. M. (2017). Methane Dehydroaromatization by Mo/HZSM-5: Mono- or Bifunctional Catalysis? *ACS Catal.* **7**, 520-529.
19. Zhang, J., Qian, W., Kong, C., Wei, F. (2015). Increasing para-Xylene Selectivity in Making Aromatics from Methanol with a Surface-Modified Zn/P/ZSM-5 Catalyst. *ACS Catal.* **5**, 2982-2988.

20. Xiao, H., Zhang, J., Wang, X., Zhang, Q., Xie, H., Han, Y., Tan, Y. (2015). A highly efficient Ga/ZSM-5 catalyst prepared by formic acid impregnation and in situ treatment for propane aromatization. *Catal. Sci. Technol.* **5**, 4081-4090.
21. Baltés, C., Vukojević, S., Schüth, F. (2008). Correlations between synthesis, precursor, and catalyst structure and activity of a large set of CuO/ZnO/Al₂O₃ catalysts for methanol synthesis. *J. Catal.* **258**, 334-344.
22. van den Berg, R., Prieto, G., Korpershoek, G., van der Wal, L. I., van Bunningen, A. J., Lægsgaard-Jørgensen, S., de Jongh, P. E., de Jong, K. P. (2016). Structure sensitivity of Cu and CuZn catalysts relevant to industrial methanol synthesis. *Nat. Commun.* **7**, 13057.
23. Sun, J., Zhu, K., Gao, F., Wang, C., Liu, J., Peden, C. H. F., Wang, Y. (2011). Direct Conversion of Bio-ethanol to Isobutene on Nanosized Zn_xZr_yO_z Mixed Oxides with Balanced Acid-Base Sites. *J. Am. Chem. Soc.* **133**, 11096-11099.
24. Jiao, F., Li, J., Pan, X., Xiao, J., Li, H., Ma, H., Wei, M., Pan, Y., Zhou, Z., Li, M., Miao, S., Li, J., Zhu, Y., Xiao, D., He, T., Yang, J., Qi, F., Fu, Q., Bao, X. (2016). Selective conversion of syngas to light olefins. *Science* **351**, 1065-1068.
25. Choi, M., Cho, H. S., Srivastava, R., Venkatesan, C., Choi, D. H., Ryoo, R. (2006). Amphiphilic organosilane-directed synthesis of crystalline zeolite with tunable mesoporosity. *Nat. Mater.* **5**, 718-723.
26. Li, Y., Qi, F. (2010). Recent Applications of Synchrotron VUV Photoionization Mass Spectrometry: Insight into Combustion Chemistry. *Acc. Chem. Res.* **43**, 68-78.
27. Wang, Y., Huang, Q., Zhou, Z., Yang, J., Qi, F., Pan, Y. (2015). Online Study on the Pyrolysis of Polypropylene over the HZSM-5 Zeolite with Photoionization Time-of-Flight Mass Spectrometry. *Energy & Fuels* **29**, 1090-1098.